Exploitation of Guest Accessible Aliphatic Amine Functionality of a Metal–Organic Framework for Selective Detection of 2,4,6- Trinitrophenol (TNP) in Water

ARTICLE *in* CRYSTAL GROWTH & DESIGN · AUGUST 2015

Impact Factor: 4.89 · DOI: 10.1021/acs.cgd.5b00902

5 AUTHORS, INCLUDING:

Soumya Mukherjee
Indian Institute of Science Education and Re…

30 PUBLICATIONS **246** CITATIONS

SEE PROFILE

CRYSTAL GROWTH & DESIGN

Article

pubs.acs.org/crystal

Exploitation of Guest Accessible Aliphatic Amine Functionality of a Metal−Organic Framework for Selective Detection of 2,4,6-Trinitrophenol (TNP) in Water

Soumya Mukherjee, Aamod V. Desai, Biplab Manna, Arif I. Inamdar, and Sujit K. Ghosh*

Indian Institute of Science Education and Research (IISER), Dr. Homi Bhabha Road, Pashan, Pune-411008, India

Supporting Information

ABSTRACT: Highly selective and sensitive aqueous phase-detection of the well-known nitro explosive environmental pollutant 2,4,6-trinitrophenol (TNP) by a water-stable, porous luminescent metal−organic framework has been reported. The presence of a guest accessible aliphatic amine functionality in the MOF channels has been strategically harnessed for serving the purpose of exclusive TNP-sensing in water even in concurrent presence of other nitro aromatic and nitro aliphatic analytes.

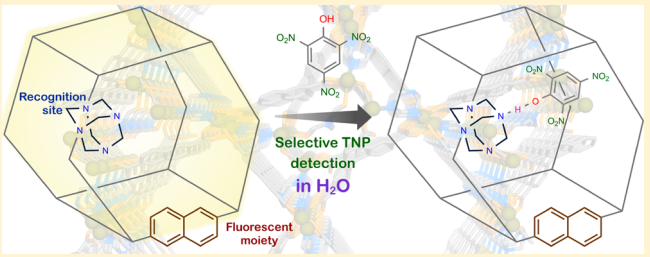

INTRODUCTION

Selective and sensitive detection of lethal explosive toxins has become one of the prime challenges from the ubiquitously vital perspectives of national/international safety and homeland security in order to tackle antiterrorist operations for civilian safety.[1−6] Nitro aromatics (NACs), like 2,4,6-trinitrotoluene (TNT), 2,4-dinitrotoluene (2,4-DNT), 2,6-dinitrotoluene (2,6-DNT), 2,4,6- trinitrophenol (TNP), or picric acid (PA), along with nitro aliphatic compounds like 1,3,5- trinitro-1,3,5-triazacyclohexane (RDX), explosive tag 2,3-dimethyl-2,3-dinitrobutane (DMNB), and nitromethane (NM), are the most commonplace constituents of the vast spectra of the human-deployed explosive substances.[4,5,7,8] As a related matter of fact, TNP has superior explosive efficacy in this class of explosives (even more than TNT), which results in its extensive usage in landmines over the past few decades.[9−12] Strikingly enough, apart from the widespread recognition of its explosive power; the one attribute which makes TNP even more dangerous is its mutagenic activities leading to acute health disorders like skin/eye irritation, headache, anemia, liver injury, male infertility, and so forth.[13−15] Moreover, this can simultaneously result in catastrophic environmental pollution owing to its high water-solubility while being widely used in numerous industries, especially leather, pharmaceutical, and dye industries, or in explosive devices and rocket fuels.[16] The widespread usage of TNP in these multifarious industrial protocols has led to toxic industrial waste effluents polluting nearby soil and aquatic system causing severe health hazards.[10−12] The anticipated effects of TNP-contamination such as allergic reactions coupled with strong irritation become even more magnified and way beyond control, because of its minimal biodegradability stemming from its inherently high electron deficient nature.[17,18] Hence, rapid and selective detection of trace amounts of TNP present in soil and aquatic systems adjacent to chemical industries or explosive-affected regions, and detecting buried unexploded ordnance and locating underwater mines, is a pressing issue targeted at apposite environmental monitoring to tackle TNP-triggered contagious aftereffects.[19,20] However, selective and sensitive detection of aqueous contaminant TNP in the presence of competing nitro analytes poses a great challenge, in view of the said analyte's high electron affinity facilitating a false response.[21−23]

Current explosive detection methods including trained canines and modern analytical techniques such as high-pressure liquid chromatography,[24] surface-enhanced Raman spectroscopy,[25] amperometry,[26] energy-dispersive X-ray analysis,[27] electrochemistry,[28] and cyclic voltammetry,[29] although significant, suffer from common drawbacks like cumbersome pretreatment of samples, interference from other compounds, low sensitivity, high operational cost, sophisticated instrumentation, and portability issues during in-field use.[2,24] On the flipside, fluorescent probe based methods harnessed from photoluminescence (PL)-based chemosensors possess unparalleled sensitivity, selectivity, low instrumentation cost, portability, short response time, and dual compatibility in solid and solution media.[5,30−32]

Several luminescent probes have been explored as fluorescence-based explosive-sensors recently,[12,22,33−50] but their multistep processing, toxicity, and lack of control over molecular organization limits their wide use.[8,51] In fact, literature reports on fluorophore probe-based explosive sensing in water have indeed been scarce.[32,35,52−56] In this regard, instead of solubilization of the probe, water-stability is a unique feature exhibited by some of the new-generation functional materials like metal−organic frameworks (MOFs),[57−60] where-

Received: June 30, 2015
Revised: July 29, 2015

DOI: 10.1021/acs.cgd.5b00902
Cryst. Growth Des. XXXX, XXX, XXX−XXX

Scheme 1. Schematic Representation of the Intermolecular H-Bonding Driven TNP-Selective Fluorescence Quenching Response for Ur-MOF

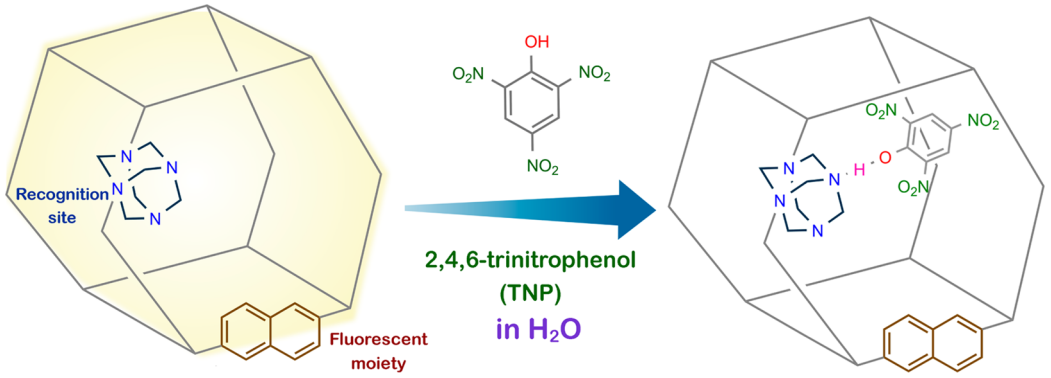

in the inherent porous framework remains unaffected in water, even after prolonged exposure to the specific water-stable MOFs. Apart from their well-recognized multifarious applications in the microporous domain,[61−78] MOFs have established themselves as excellent sensory materials because of the unmatched combination of crystallinity, permanent porosity, and designable pores with tailored window-sizes, systematically tunable band gaps, and electronic structures.[79−85] In general, favorable interactions between the target analyte and MOF backbone result into the observed PL-sensing performance for MOFs. While porous channels permit the crucial host−guest interactions between guest analyte and host MOF matrices, designability of pore size/shape allows an optimum molecular sieving effect in order to let the pendant recognition sites of the porous adsorbent have selective interplay with the targeted analyte. This can happen via diverse modes of favorable interactions such as H-bonding and Mülliken-type interactions along with the effect of Lewis acid−base sites and open metal sites, resulting in the selective accumulation of the targeted analyte in the MOF matrix giving rise to enhanced sensing performance, commonly denoted as the preconcentration effect.[85] Moreover, the immobilization of organic linkers in MOFs results in a superior emission signature owing to reduced nonradiative relaxation. Additionally, myriad choices of organic linkers and metal clusters/centers allow tuning of valence and/or conduction band and consequently the band gap, crucial for electronic property-driven sensing applications. Furthermore, strategic introduction of secondary functional group(s) gives rise to favored binding of the chosen analyte to the respective probe framework, giving rise to better selectivity. These features result in the rational design and study of MOF materials for the desired selective detection of cations, anions, small molecules, explosives, and biomolecules.[13,48,80,86−99]

In view of the targeted selective TNP detection in water by MOFs with high sensitivity, regardless of the latest advances, reports of fluorescent MOFs exhibiting selective and sensitive TNP detection in the concurrent presence of other nitro analytes are few, while most of the reported MOFs involve detection only in organic/organic−water mixture phase.[86] Subsequent to the discovery of the key role of Lewis basic pyridyl functionality behind selective aqueous-media TNP sensing,[88] as a first-of-its kind approach, very recently, our group came up with two reports of aqueous phase selective TNP-sensing based on two different MOF compounds.[87,89] Therein, the origin behind the remarkable TNP-selectivity in water could be indubitably attributed to the presence of strong intermolecular H-bonding-assisted favorable interactions between the free functional amine moieties decorating the porous matrix of the MOFs and the nitrophenolic analyte TNP. For both these instances, employment of guest-accessible free amino Lewis basic sites for accomplishing the desired TNP selectivity in water was the key feature. Herein, instead of probing into the primary amino groups ($-NH_2$) as the active pendant sites (Scheme 1),[100] in order to further delve into the amine−TNP H-bonding mediated selective TNP sensing phenomena, and to improve the sensitivity/selectivity, Lewis basic tertiary aliphatic amine functionality of constituent linker urotropine (Ur) has been chosen as the probe under focus in a rationally selected water-stable luminescent microporous MOF (hereinafter, denoted as Ur-MOF).[101] In this report, we have envisaged Ur-MOF as the luminescent probe, considering its superb facets, comprising an exceptional combination of permanent porosity, rigidity, water stability, luminescence property, and free functional guest-accessible tertiary amine groups decorating the void channels.

EXPERIMENTAL SECTION

Materials and Measurements. *Materials.* TNT and RDX were obtained from HEMRL Pune (India). TNP, NB, 2,4-DNT, 2,6-DNT, DMNB, and NM were procured from Aldrich and used as received. Dry solvents were carefully used during entire analyses.

Caution: TNT, RDX, and TNP are highly explosive and should be handled carefully and in small amounts. The explosives should be handled as dilute solutions and with safety measures to avoid an explosion.

Physical Measurements. X-ray powder pattern was recorded on Bruker D8 Advanced X-ray diffractometer at room temperature using Cu Kα radiation (λ = 1.5406 Å). Thermogravimetric analyses were obtained in the temperature range of 30−800 °C on PerkinElmer STA 6000 analyzer under a N_2 atmosphere at a heating rate of 10 °C min^{-1}. Fluorescence measurements were done using Horiba FluoroMax 4 with stirring attachment.

X-ray Structural Studies. Single-crystal X-ray data were collected at 100 K on a Bruker KAPPA APEX II CCD Duo diffractometer (operated at 1500 W power: 50 kV, 30 mA) with graphite-monochromated Mo Kα radiation (λ = 0.71073 Å). Crystals ware on nylon CryoLoops (Hampton Research) with Paraton-N (Hampton Research). The data integration and reduction were processed with SAINT[102] software. A multiscan absorption correction was applied to the collected reflections. The structures ware solved by the direct method using SHELXTL[103] and was refined on F^2 by full-matrix least-squares technique using the SHELXL-97[104] program package within the WINGX[105] program. All non-hydrogen atoms were refined anisotropically. All hydrogen atoms were located in successive difference Fourier maps and were treated as riding atoms using

DOI: 10.1021/acs.cgd.5b00902
Cryst. Growth Des. XXXX, XXX, XXX−XXX

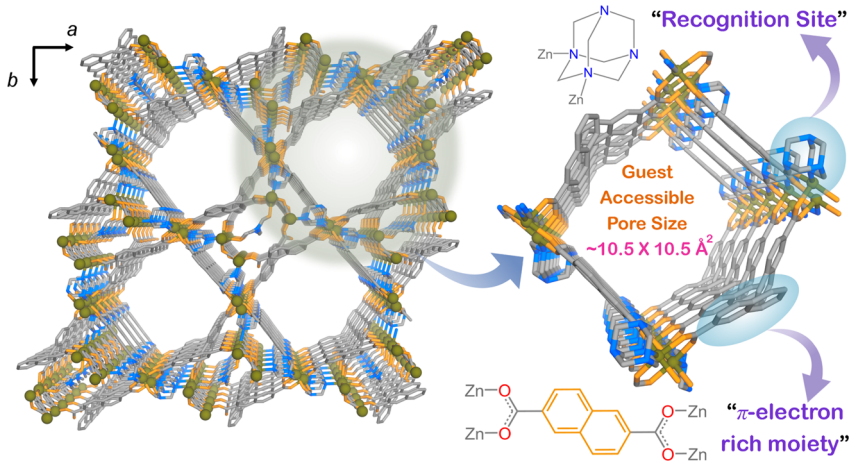

Figure 1. (a) Perspective view of three-dimensional porous framework of Ur-MOF along the crystallographic *c* axis. (b) Perspective view of each of the single one-dimensional channels decorated with fluorescent π-electron rich naphthalene moieties along with guest-accessible tertiary functional aliphatic amino groups. Hydrogen atoms are omitted for clarity.

SHELXL default parameters. The structures were examined using the *Adsym* subroutine of PLATON[106] to ensure that no additional symmetry could be applied to the models.

Synthesis of Ur-MOF. Synthesis of Ur-MOF was done according to the following synthetic protocol, which was somewhat distinct compared to the one reported in the literature followed by Samsonenko et al.:[101] 3 mL DMF solution of a mixture of $Zn(NO_3)_2{\cdot}6H_2O$ (0.1 mM), 2,6-Naphthalenedicarboxylic acid (0.1 mM) and Urotropine (0.1 mM) was heated at 100 °C for 24 h, followed by slow cooling (3 °C min^{-1}) to obtain colorless, shiny block-shaped single crystals of Ur-MOF⊃G. Anal. Found (%): C 50.1; H 5.4; N 10.3. These crystals of were kept immersed in dried CH_2Cl_2 for 72 h with periodic change of the supernatant solution twice a day to obtain the DCM-exchanged phase, which was subsequently heated under vacuum at 80 °C for 8 h, to end up with colorless guest-free desolvated crystalline phase Ur-MOF. Anal: Found (%): C 51.7; H 3.6; N 8.8.

Synthesis of Co-Crystal 1. One mL DCM solution of urotropine (35 mg, 0.025 mM) was dispensed into a glass tube. Cyclohexane (1 mL) was poured onto this Ur-solution, followed by slow layering of a 1 mL methanolic solution of 2,4,6-trinitrophenol (5.7 mg, 0.025 mmol). Clean, pale yellow colored block-shaped crystals suitable for X-ray analysis were obtained after 5 days in 80% yield.

Fluorescence Study. One mg of desolvated guest-free crystals of Ur-MOF (ground well by mortar−pestle) is weighed and added to a fluorescence cuvette (path length of 1 cm), containing 2 mL of Milli-Q water under constant stirring. The photoluminescence spectral response in 350−530 nm range upon excitation at 310 nm was measured in situ, after incremental addition of freshly prepared aqueous analyte solutions (1 mM each; 20−200 μL) and corresponding fluorescence intensities were monitored at 400 nm. All PL-spectra have been recorded under continuous stirring by the fluorescence instrument's stirrer setup accessory.

Low Pressure Gas Sorption Measurements. Low pressure N_2 sorption measurement was performed using BelMax (Bel Japan). The gas used was of 99.999% purity. Prior to adsorption measurement, the guest free sample Ur-MOF was pretreated at 100 °C under vacuum for 4 h, using BelPrepvacII, and purged with N_2 on cooling.

RESULTS AND DISCUSSION

Even though MOF-engineering and pore-window manipulation always involves some extent of certainty, guessing the pore surface properties is indeed challenging. Conversely, quite a large number of MOFs have been reported that can potentially be utilized for multifarious sensing applications. The approach of purposefully using the Cambridge Structural Database (CSD) is steadily receiving escalating attention to find potential compounds with targeted properties. Using the CSD-based approach, we screened MOF compounds looking for the targeted property of aqueous-phase detection of TNP by the intermediacy of intermolecular H-bonding between aliphatic amine and the nitrophenolic explosive analyte, which resulted in finding a Zn(II)-naphthalenedicarboxylate based urotropine (Ur)-linker functionalized three-dimensional microporous guest-free MOF (Ur-MOF) $[Zn_4(DMF)\ (Ur)_2(NDC)_4]$ (NDC = 2,6-naphtalenedicarboxylic acid, Ur = urotropin, DMF = *N*,*N*-dimethylformamide) as the most suitable luminescent probe-candidate. Ur-MOF, in addition to the desired presence of the functional prerequisites, also possesses a substantially large 1D channel (ca. 10.5 × 10.5 $Å^2$) along the crystallographic *c*-axis (Figure 1). This should, in principle, enable concentration and consequent interaction-driven accumulation of nitro analytes in MOF matrix (Table S4). These pore windows are precisely decorated with the guest accessible pendant aliphatic amine moieties (Figure 1b) which might act as recognition sites for TNP, giving rise to efficient PL-quenching response.

The aforementioned probe was solvothermally synthesized using Zn^{2+} and the employment of mixed ligand combination of luminescent NDC and Lewis basic aliphatic N-containing Ur ligands (described in the Experimental section). The tertiary nitrogen-Lewis basic sites and naphthalene moiety-functionalized symmetric hexagonal channels running along the *c*-axis render Ur-MOF to be substantially porous, as evidenced from ~43% void volume (probe radius = 1.2 Å) in PLATON analysis, and the microporosity-characteristic Type-I N_2 adsorption isotherm registered at 77 K (Figure S3). The evidence of permanent microporosity for the bulk Ur-MOF suggests the feasibility of nitro explosive analytes to gain entry inside the pores for the site-specific interactions to occur with the functionalized porous channels.

Powder-X-ray diffraction (PXRD) studies revealed its excellent crystalline feature, along with its phase purity (Figure S1). Additionally, thermogravimetric analyses came up with a typically stable thermogram (Figure S2), clearly providing the indication of a thermally stable phase, obtained on activating the DCM-exchnaged phase of Ur-MOF⊃G at ~80 °C under vacuum, with nearly similar PXRD profile as observed for the parent as-synthesized Ur-MOF⊃G. Therefore, the phase purity

DOI: 10.1021/acs.cgd.5b00902
Cryst. Growth Des. XXXX, XXX, XXX−XXX

and guest-free nature for the desolvated phase (Ur-MOF) once confirmed, for targeting practical aqueous-phase sensing applications, water stability for Ur-MOF was also verified by PXRD analysis (Figure 2). Interestingly, Ur-MOF presented

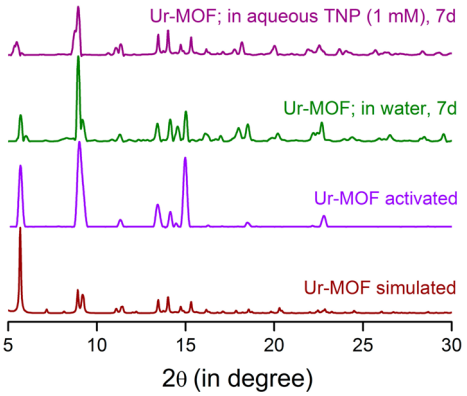

Figure 2. Phase purity and aqueous stability validation by PXRD analyses of different phases of Ur-MOF, compared with the simulated one.

excellent hydrolytic stability as anticipated,[107−112] owing to its hydrophobic naphthalene moieties (Figure 2), which further encouraged us to comprehensively investigate its selective trace-amount TNP-sensing performance in water.

Guest-free crystals of Ur-MOF when dispersed in water presented a strong fluorescence-signature upon excitation at 310 nm. To ascertain the nitro explosive sensing ability of Ur-MOF in water, fluorescence intensities of this probe dispersed in water were monitored upon addition of aqueous solutions (10^{-3} M; 20−200 μL each) of different aromatic nitro explosives like TNP, 2,4-DNT, 2,6-DNT, TNT, and NB and nitro aliphatic explosives such as RDX, DMNB, and NM (Figures 3 and S5−S11). As anticipated, the incremental addition of TNP resulted in rapid and efficient fluorescence quenching response of ∼98% (on addition of 1 mM, 200 μL aqueous TNP solution; 25 °C) (Figure 3a).

The PL-quenching driven recognition for TNP could be determined exactly at as low as 1.63 ppm concentration (parts per million) or 7.1 μM (Figure S18, Tables S1−S2). Strikingly enough, this TNP-detection limit is found to be comparable to/or superior than the previous MOF reports in the domain of selective TNP detection.[48] In contrast, all the other competing nitro analytes came up with only minuscule effects on the emission intensity of Ur-MOF (Figure 3b). These results clearly reveal the high selectivity of Ur-MOF toward TNP in comparison to potentially interfering nitro analytes.

The discriminating effect of TNP addition on the fluorescence signatures of aqueous dispersions of Ur-MOF, happening during the PL-quenching experiments, could easily be monitored under UV-irradiation (λ_{max} = 365 nm), wherein the turn-off response on addition of 200 μL of analyte to 2 mL water-dispersion of 1 mg Ur-MOF could be clearly distinguished for TNP (Figure 4).

To further quantify the selective TNP-mediated PL-quenching competence, Stern−Volmer (SV) plots of the relative PL intensities (I_0/I) of all the nitro analytes were precisely judged against each other, where I_0 and I are the corresponding intensities in the absence and in the presence of the relevant nitro analytes (Figure 5). The typical nonlinear nature of the SV plot was solely encountered for TNP, while

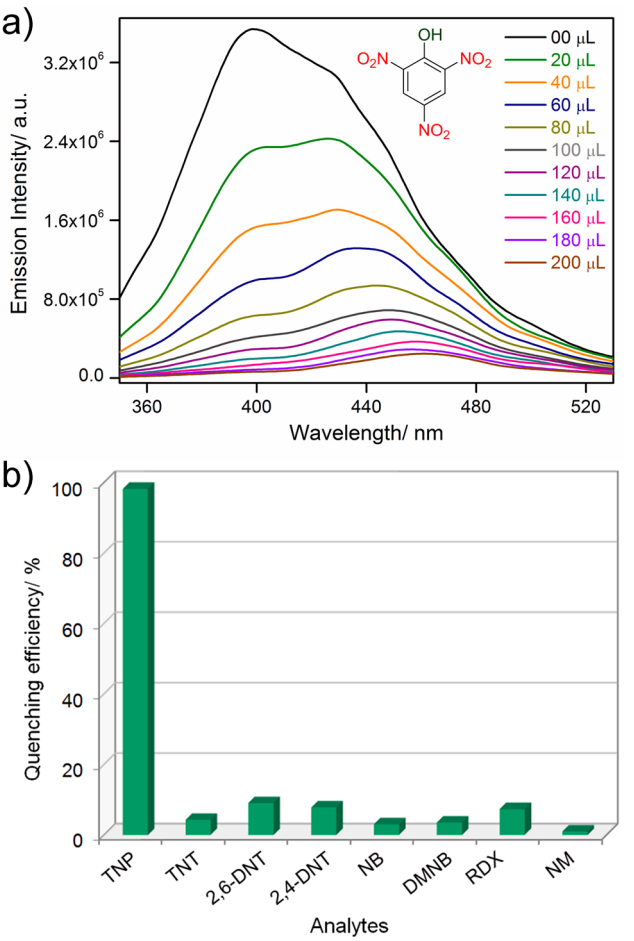

Figure 3. (a) Emission spectra of luminophore probe (Ur-MOF) dispersed in water, upon incremental addition of aqueous TNP solution (1 mM). (b) Quenching efficiency plot (bar diagram) for different nitro analytes in the case of compound Ur-MOF.

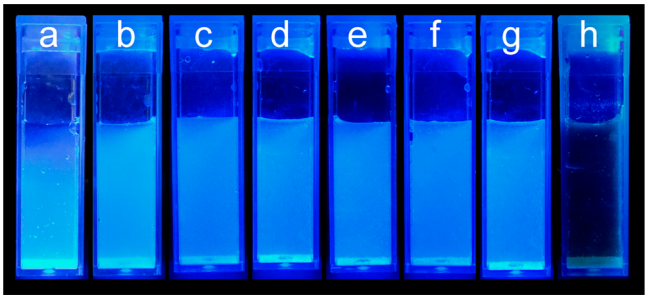

Figure 4. Response of Ur-MOF aqueous dispersions (1 mg in 2 mL water) toward the additions of various nitro analyte aqueous solutions (200 μL each) under UV light (λ_{max} = 365 nm) (a = TNT, b = NM, c = RDX, d = 2,4-DNT, e = 2,6-DNT, *f* = NB, g = DMNB, h = TNP).

others register linear SV signatures. As a more captivating matter of fact, a linear SV plot was the outcome for low concentrations of TNP, while a slightly nonlinear feature was observed at higher concentrations. This observed nonlinearity of the SV plot particularly in the case of TNP indisputably suggests the simultaneous attendance of both dynamic and static quenching processes and/or the occurrence of an energy-transfer phenomenon between Ur-MOF and TNP.[49,113,114] The quenching constant (K_D) for TNP, calculated from the SV plot, was found to be 10.83 × 10^4 M^{-1} (0−0.04 mM; Figure

DOI: 10.1021/acs.cgd.5b00902
Cryst. Growth Des. XXXX, XXX, XXX−XXX

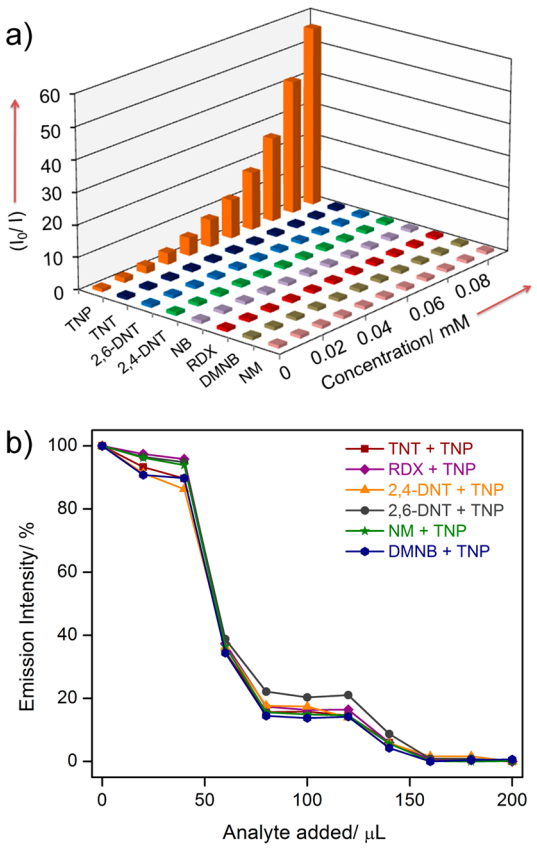

Figure 5. (a) Stern−Volmer plots for all the nitro analytes in water ([Ur-MOF] = 1 mg/2 mL). (b) Photoluminescence quenching response of Ur-MOF, upon addition of aqueous solutions of different nitro explosive analytes followed by TNP (1 mM; 20 μL batches for two consecutive times in each occurrence).

S17). The observed quenching constant for TNP is equivalent to those of organic polymer-based probes and is ∼100 times higher than those of its non-phenolic aromatic trinitro-analogue TNT and aliphatic trinitro-analogue RDX, demonstrating the outstanding selective TNP-detection performance in water, crucial for environmental monitoring.

To gain better comprehension of the selective TNP-sensing ability of Ur-MOF, we sought to examine the electronic properties of both the MOF and nitro analyte probes. Fluorescence quenching by electron transfer from the conduction band (CB) of the MOF to LUMO orbitals of the electron-deficient nitro analytes is an established quenching mechanism.[4,115] Generally, the conduction band (CB) of electron-rich MOF lies higher as compared to the LUMO energies of electron-deficient nitro analytes, and upon excitation the excited electron from CB transfers to the LUMO orbitals of nitro analytes, consequently resulting in PL-intensity quenching. As the LUMO energy gets smaller, the electron accepting efficiency of the nitro analytes increases, along with the fluorescence quenching performance. The observed selective fluorescence quenching by TNP is in splendid agreement with its LUMO energy value being lower than those for all other nitro analytes, as calculated by density functional theory at the B3LYP/6-31G* level (Figure S15). Nevertheless, the PL-quenching for all other nitro analytes except TNP is not in exact accordance with their LUMO energy trend, suggesting the synchronous presence of other quenching mechanisms involved along with electron transfer. Resonance energy transfer is one more effective fluorescence quenching mechanism, often ascribed for such PL-quenching responses.[86−88] In fact, the nonlinear SV plot for TNP substantiates the presence of long-range resonance energy transfer. The effectiveness of the energy transfer significantly relies on the extent of spectral overlap between the emission spectra of the fluorophore and the absorption spectra of the concerned nonemissive analyte. With energy transfer phenomenon being a long-range process, the PL-quenching response can pass on to the surrounding fluorophores quite efficiently.

Herein, the absorption spectrum for TNP exhibits a massive overlap with the MOF emission spectrum, as compared to the competing nitro analytes where there is almost no such overlap (Figure S16). This is in reasonable agreement with the observed superior quenching efficiency encountered for TNP than the other nitro explosive analytes. Therefore, it is prominent in the case of TNP that both electron- and energy-transfer mechanisms are operational while other nitro analytes could employ merely electron-transfer mechanism. As a result of the combined involvement of such processes, namely, electron-transfer and energy-transfer processes, the quenching efficiency of TNP might have undergone the observed enhancement, magnifying the selectivity limits as well as yielding a good detection-sensitivity limit.

Motivated form these observations, the selectivity of Ur-MOF toward TNP even in the concurrent presence of other nitro-analytes was comprehensively investigated by competing nitro-analyte test (CNA test: Figure 5b).[86−88] Following standard verification protocol, the PL spectrum for water-dispersed Ur-MOF was recorded upon the incremental consecutive addition of a 1 mM aqueous solution of TNT (40 μL in two evenly distributed batches), to allow high-affinity basic −N− sites in the surface of Ur-MOF to become accessible to guest analyte TNT, which merely led to a minute PL-quenching effect. More fascinatingly, subsequent TNP (40 μL, 1 mM aqueous solution) addition resulted in a strikingly prompt and noteworthy PL-quenching response, with a precisely alike trend observed in the following repeat cycles of TNT and TNP additions performed in the same chronological order (Figure 5b). Addition of aqueous solutions of all the congener series of nitro analyte analogues followed by TNP to Ur-MOF also ended up with the similar CNA-plot trend, reaffirming exclusive TNP-selectivity, even in the simultaneous presence of other nitro explosive species.

In the literature, TNP is recognized to interact favorably with Lewis basic sites owing to its acidic phenolic proton.[100] To probe the role of the pendant Lewis basic free aliphatic amines of Ur-linker behind the observed selectivity, PL-quenching titrations were performed with analogous nitrophenolic analytes 2,4-dinitrophenol (2,4-DNP) and 4-nitrophenol (NP). The PL-quenching order nicely coincides with the decreasing acidity sequence of the phenolic protons of the analytes: TNP > 2,4-DNP > NP (Figure S14). This matching trend indicates the presence of electrostatic interactions between TNP and the pendant amine functionality, similar to that prevalent for the pyridyl functionalized MOFs.[89] The most acidic TNP selectively and favorably interacts with the pendant Lewis basic aliphatic amine groups via hydrogen-bonding and ionic interactions, resulting in an amplified turn-off PL-response. Thus, the Lewis basic aliphatic amine functionality functions as recognition site for TNP, and a cooperative effect of both electron-transfer and energy-transfer quenching

DOI: 10.1021/acs.cgd.5b00902
Cryst. Growth Des. XXXX, XXX, XXX−XXX

mechanisms in unison leads to the desired TNP-selectivity in water.

To deteremine the basic principle operating behind this encountered exclusive selectivity of Ur-MOF toward TNP, a possible quenching mechanism was sought. In the absence of the explicit evidence of TNP loaded Ur-MOF crystal because of weak diffraction nature, a co-crystal of TNP and the functional co-ligand (urotropine) was obtained by slow diffusion at room temperature (for method, see Experimental section). Single-crystal X-ray diffraction (SC-XRD) studies disclosed that the desired co-crystal crystallized in monoclinic $P2_1/c$ space group as [(urotropine) (TNP)], the same as reported recently by Singh et al. (Figure 6).[116] As anticipated, the free tertiary

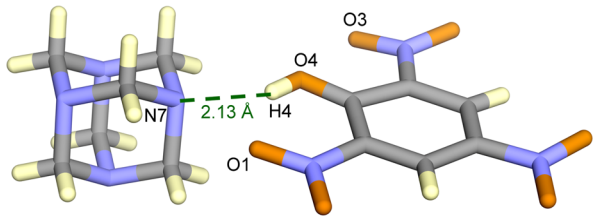

Figure 6. SC-XRD structure of the co-crystal **1** of urotropine (Ur) and TNP revealing intermolecular H-bonding interactions (color code: gray, carbon; blue, nitrogen; dark yellow, oxygen; faint yellow, hydrogen).

aliphatic amine group of urotropine forms a cooperative intermolecular hydrogen-bonded complex with TNP. Such intermolecular H-bonding interaction-driven facile diffusion of TNP inside the aliphatic nitrogen decorated MOF channels amplify the feasible host–guest interactions, leading to an excellent sensitive response during the selective interplay of TNP with Ur-MOF.

CONCLUSION

In conclusion, the distinctive blend of aliphatic amine-functionalized porous channels and hydrolytic stability renders nitro explosive TNP-selectivity to the purposefully chosen luminescent Zn(II)-naphthalenedicarboxylate Ur-MOF in aqueous media, even in the concurrent presence of all other nitro analytes. The cooperative unison of the ionic interactions between tertiary aliphatic amine decorated pores with TNP and the facilitated electron- and energy-transfer processes endow Ur-MOF with an exceptionally selective luminescence-quenching efficiency for TNP, registering substantial sensitivity and detection limits in water. Demonstrating the potential of suitably functionalized luminescent MOFs for sensing applications, the present work describes the best selectivity results (~98% quenching for TNP) for real-time aqueous-media nitro explosive detection in the MOF and porous materials' domain, aimed at practical security and environmental applications. It seems promising to judiciously extend and improve the strategy adopted herein in order to obtain even better explosive sensors for real-time sensing applications in the near future.

ASSOCIATED CONTENT

Supporting Information

The Supporting Information is available free of charge on the ACS Publications website at DOI: 10.1021/acs.cgd.5b00902.

PXRD, TGA, Excitation and Emission spectra, Quenching-efficiency plot, HOMO and LUMO energies, Stern-Volmer (SV) plots, Crystal data and structure refinement. (PDF)

AUTHOR INFORMATION

Corresponding Author

*E-mail: sghosh@iiserpune.ac.in. Fax: +91 20 2590 8186.

Author Contributions

The manuscript was written through contributions of all authors.

Notes

The authors declare no competing financial interest.

ACKNOWLEDGMENTS

S.M. and A.V.D. are thankful to IISER Pune for research fellowships. B.M. and A.I.I. thank CSIR and SERB (Project No.: 30112083) respectively for the same. We are grateful to IISER Pune for research facilities. DST (Project No. GAP/DST/CHE-12-0083) is acknowledged for the financial support. DST-FIST (SR/FST/CSII-023/2012) is acknowledged for microfocus SC-XRD facility.

REFERENCES

(1) Yang, J.-S.; Swager, T. M. *J. Am. Chem. Soc.* **1998**, *120*, 11864–11873.
(2) Sohn, H.; Sailor, M. J.; Magde, D.; Trogler, W. C. *J. Am. Chem. Soc.* **2003**, *125*, 3821–3830.
(3) McQuade, D. T.; Pullen, A. E.; Swager, T. M. *Chem. Rev.* **2000**, *100*, 2537–2574.
(4) Toal, S. J.; Trogler, W. C. *J. Mater. Chem.* **2006**, *16*, 2871–2883.
(5) Germain, M. E.; Knapp, M. J. *Chem. Soc. Rev.* **2009**, *38*, 2543–2555.
(6) Thomas, S. W.; Joly, G. D.; Swager, T. M. *Chem. Rev.* **2007**, *107*, 1339–1386.
(7) Meaney, M.; McGuffin, V. *Anal. Bioanal. Chem.* **2008**, *391*, 2557–2576.
(8) Salinas, Y.; Martinez-Manez, R.; Marcos, M. D.; Sancenon, F.; Costero, A. M.; Parra, M.; Gil, S. *Chem. Soc. Rev.* **2012**, *41*, 1261–1296.
(9) He, G.; Peng, H.; Liu, T.; Yang, M.; Zhang, Y.; Fang, Y. *J. Mater. Chem.* **2009**, *19*, 7347–7353.
(10) Venkatramaiah, N.; Kumar, S.; Patil, S. *Chem. Commun.* **2012**, *48*, 5007–5009.
(11) Peng, Y.; Zhang, A.-J.; Dong, M.; Wang, Y.-W. *Chem. Commun.* **2011**, *47*, 4505–4507.
(12) Dong, M.; Wang, Y.-W.; Zhang, A.-J.; Peng, Y. *Chem. - Asian J.* **2013**, *8*, 1321–1330.
(13) Thorne, P. G.; Jenkins, T. F. *Field Anal. Chem. Technol.* **1997**, *1*, 165–170.
(14) Wollin, K. M.; Dieter, H. H. *Arch. Environ. Contam. Toxicol.* **2005**, *49*, 18–26.
(15) Wyman, J. F.; Serve, M. P.; Hobson, D. W.; Lee, L. H.; Uddin, D. E. *J. Toxicol. Environ. Health* **1992**, *37*, 313–327.
(16) Akhavan, J. *The Chemistry of Explosives*; Royal Society of Chemistry: Cambridge, 2004; p 4.
(17) Shen, J.; Zhang, J.; Zuo, Y.; Wang, L.; Sun, X.; Li, J.; Han, W.; He, R. *J. Hazard. Mater.* **2009**, *163*, 1199–1206.
(18) Shen, J.; He, R.; Yu, H.; Wang, L.; Zhang, J.; Sun, X.; Li, J.; Han, W.; Xu, L. *Bioresour. Technol.* **2009**, *100*, 1922–1930.
(19) Toal, S. J.; Magde, D.; Trogler, W. C. *Chem. Commun.* **2005**, 5465–5467.
(20) Shriver-Lake, L. C.; Donner, B. L.; Ligler, F. S. *Environ. Sci. Technol.* **1997**, *31*, 837–841.
(21) Xu, B.; Wu, X.; Li, H.; Tong, H.; Wang, L. *Macromolecules* **2011**, *44*, 5089–5092.
(22) Chowdhury, A.; Mukherjee, P. S. *J. Org. Chem.* **2015**, *80*, 4064–4075.

DOI: 10.1021/acs.cgd.5b00902
Cryst. Growth Des. XXXX, XXX, XXX–XXX

(23) Rong, M.; Lin, L.; Song, X.; Zhao, T.; Zhong, Y.; Yan, J.; Wang, Y.; Chen, X. *Anal. Chem.* **2015**, *87*, 1288−1296.
(24) Moore, D. S. *Rev. Sci. Instrum.* **2004**, *75*, 2499−2512.
(25) Sylvia, J. M.; Janni, J. A.; Klein, J. D.; Spencer, K. M. *Anal. Chem.* **2000**, *72*, 5834−5840.
(26) Hilmi, A.; Luong, J. H. T. *Anal. Chem.* **2000**, *72*, 4677−4682.
(27) Luggar, R. D.; Farquharson, M. J.; Horrocks, J. A.; Lacey, R. J. *X-Ray Spectrom.* **1998**, *27*, 87−94.
(28) Hodyss, R.; Beauchamp, J. L. *Anal. Chem.* **2005**, *77*, 3607−3610.
(29) Krausa, M.; Schorb, K. *J. Electroanal. Chem.* **1999**, *461*, 10−13.
(30) Xin, Y.; Wang, Q.; Liu, T.; Wang, L.; Li, J.; Fang, Y. *Lab Chip* **2012**, *12*, 4821−4828.
(31) Basabe-Desmonts, L.; Reinhoudt, D. N.; Crego-Calama, M. *Chem. Soc. Rev.* **2007**, *36*, 993−1017.
(32) He, G.; Yan, N.; Yang, J.; Wang, H.; Ding, L.; Yin, S.; Fang, Y. *Macromolecules* **2011**, *44*, 4759−4766.
(33) Naddo, T.; Che, Y.; Zhang, W.; Balakrishnan, K.; Yang, X.; Yen, M.; Zhao, J.; Moore, J. S.; Zang, L. *J. Am. Chem. Soc.* **2007**, *129*, 6978−6979.
(34) Richardson, S.; Barcena, H. S.; Turnbull, G. A.; Burn, P. L.; Samuel, I. D. W. *Appl. Phys. Lett.* **2009**, *95*, 063305.
(35) Li, D.; Liu, J.; Kwok, R. T. K.; Liang, Z.; Tang, B. Z.; Yu, J. *Chem. Commun.* **2012**, *48*, 7167−7169.
(36) Andrew, T. L.; Swager, T. M. *J. Am. Chem. Soc.* **2007**, *129*, 7254−7255.
(37) Hughes, A. D.; Glenn, I. C.; Patrick, A. D.; Ellington, A.; Anslyn, E. V. *Chem. - Eur. J.* **2008**, *14*, 1822−1827.
(38) Gole, B.; Shanmugaraju, S.; Bar, A. K.; Mukherjee, P. S. *Chem. Commun.* **2011**, *47*, 10046−10048.
(39) Snow, E. S.; Perkins, F. K.; Houser, E. J.; Badescu, S. C.; Reinecke, T. L. *Science* **2005**, *307*, 1942−1945.
(40) Cavaye, H.; Shaw, P. E.; Wang, X.; Burn, P. L.; Lo, S.-C.; Meredith, P. *Macromolecules* **2010**, *43*, 10253−10261.
(41) Kartha, K. K.; Babu, S. S.; Srinivasan, S.; Ajayaghosh, A. *J. Am. Chem. Soc.* **2012**, *134*, 4834−4841.
(42) Cavaye, H.; Smith, A. R. G.; James, M.; Nelson, A.; Burn, P. L.; Gentle, I. R.; Lo, S. C.; Meredith, P. *Langmuir* **2009**, *25*, 12800−12805.
(43) Swarnkar, A.; Shanker, G. S.; Nag, A. *Chem. Commun.* **2014**, *50*, 4743−4746.
(44) Das, S.; Bharadwaj, P. K. *Inorg. Chem.* **2006**, *45*, 5257−5259.
(45) Shanmugaraju, S.; Joshi, S. A.; Mukherjee, P. S. *Inorg. Chem.* **2011**, *50*, 11736−11745.
(46) Roy, B.; Bar, A. K.; Gole, B.; Mukherjee, P. S. *J. Org. Chem.* **2013**, *78*, 1306−1310.
(47) Banerjee, D.; Hu, Z.; Li, J. *Dalton Trans.* **2014**, *43*, 10668−10685.
(48) Hu, Z.; Deibert, B. J.; Li, J. *Chem. Soc. Rev.* **2014**, *43*, 5815−5840.
(49) Acharyya, K.; Mukherjee, P. S. *Chem. Commun.* **2014**, *50*, 15788−15791.
(50) Gole, B.; Song, W.; Lackinger, M.; Mukherjee, P. S. *Chem. - Eur. J.* **2014**, *20*, 13662−13680.
(51) Zhang, S.-R.; Du, D.-Y.; Qin, J.-S.; Bao, S.-J.; Li, S.-L.; He, W.-W.; Lan, Y.-Q.; Shen, P.; Su, Z.-M. *Chem. - Eur. J.* **2014**, *20*, 3589−3594.
(52) Xu, Y.; Li, B.; Li, W.; Zhao, J.; Sun, S.; Pang, Y. *Chem. Commun.* **2013**, *49*, 4764−4766.
(53) Ding, L.; Bai, Y.; Cao, Y.; Ren, G.; Blanchard, G. J.; Fang, Y. *Langmuir* **2014**, *30*, 7645−7653.
(54) Yang, G.; Hu, W.; Xia, H.; Zou, G.; Zhang, Q. *J. Mater. Chem. A* **2014**, *2*, 15560−15565.
(55) Kumar, S.; Venkatramaiah, N.; Patil, S. *J. Phys. Chem. C* **2013**, *117*, 7236−7245.
(56) Mukherjee, S.; Desai, A. V.; Inamdar, A. I.; Manna, B.; Ghosh, S. K. *Cryst. Growth Des.* **2015**, *15*, 3493−3497.
(57) Burtch, N. C.; Jasuja, H.; Walton, K. S. *Chem. Rev.* **2014**, *114*, 10575−10612.
(58) Yang, Q.; Vaesen, S.; Ragon, F.; Wiersum, A. D.; Wu, D.; Lago, A.; Devic, T.; Martineau, C.; Taulelle, F.; Llewellyn, P. L.; Jobic, H.; Zhong, C.; Serre, C.; De Weireld, G.; Maurin, G. *Angew. Chem., Int. Ed.* **2013**, *52*, 10316−10320.
(59) Zhang, J.-W.; Zhang, H.-T.; Du, Z.-Y.; Wang, X.; Yu, S.-H.; Jiang, H.-L. *Chem. Commun.* **2014**, *50*, 1092−1094.
(60) Yang, J.; Grzech, A.; Mulder, F. M.; Dingemans, T. J. *Chem. Commun.* **2011**, *47*, 5244−5246.
(61) Mason, J. A.; Veenstra, M.; Long, J. R. *Chem. Sci.* **2014**, *5*, 32−51.
(62) Ma, S.; Zhou, H.-C. *Chem. Commun.* **2010**, *46*, 44−53.
(63) Wang, C.; Zhang, T.; Lin, W. *Chem. Rev.* **2012**, *112*, 1084−1104.
(64) Li, J.-R.; Kuppler, R. J.; Zhou, H.-C. *Chem. Soc. Rev.* **2009**, *38*, 1477−1504.
(65) Lee, J.; Farha, O. K.; Roberts, J.; Scheidt, K. A.; Nguyen, S. T.; Hupp, J. T. *Chem. Soc. Rev.* **2009**, *38*, 1450−1459.
(66) Zhang, Z.; Zhao, Y.; Gong, Q.; Li, Z.; Li, J. *Chem. Commun.* **2013**, *49*, 653−661.
(67) Corma, A.; García, H.; Llabrés i Xamena, F. X. *Chem. Rev.* **2010**, *110*, 4606−4655.
(68) Horcajada, P.; Serre, C.; Vallet-Regí, M.; Sebban, M.; Taulelle, F.; Férey, G. *Angew. Chem., Int. Ed.* **2006**, *45*, 5974−5978.
(69) Tanabe, K. K.; Allen, C. A.; Cohen, S. M. *Angew. Chem., Int. Ed.* **2010**, *49*, 9730−9733.
(70) Shimizu, G. K. H.; Taylor, J. M.; Kim, S. *Science* **2013**, *341*, 354−355.
(71) Yoon, M.; Suh, K.; Natarajan, S.; Kim, K. *Angew. Chem., Int. Ed.* **2013**, *52*, 2688−2700.
(72) Umeyama, D.; Horike, S.; Inukai, M.; Kitagawa, S. *J. Am. Chem. Soc.* **2013**, *135*, 11345−11350.
(73) Shigematsu, A.; Yamada, T.; Kitagawa, H. *J. Am. Chem. Soc.* **2011**, *133*, 2034−2036.
(74) Yamada, T.; Otsubo, K.; Makiura, R.; Kitagawa, H. *Chem. Soc. Rev.* **2013**, *42*, 6655−6669.
(75) Denayer, J. F. M.; De Vos, D.; Leflaive, P. Separation of Xylene Isomers. In *Metal-Organic Frameworks*; Wiley-VCH Verlag GmbH & Co. KGaA, 2011; pp 171−190.
(76) Mukherjee, S.; Joarder, B.; Manna, B.; Desai, A. V.; Chaudhari, A. K.; Ghosh, S. K. *Sci. Rep.* **2014**, *4*, DOI: 10.1038/srep05761.
(77) Chen, Y.-Z.; Zhou, Y.-X.; Wang, H.; Lu, J.; Uchida, T.; Xu, Q.; Yu, S.-H.; Jiang, H.-L. *ACS Catal.* **2015**, *5*, 2062−2069.
(78) Kitagawa, S.; Kitaura, R.; Noro, S.-i. *Angew. Chem., Int. Ed.* **2004**, *43*, 2334−2375.
(79) Lan, A.; Li, K.; Wu, H.; Olson, D. H.; Emge, T. J.; Ki, W.; Hong, M.; Li, J. *Angew. Chem., Int. Ed.* **2009**, *48*, 2334−2338.
(80) Kreno, L. E.; Leong, K.; Farha, O. K.; Allendorf, M.; Van Duyne, R. P.; Hupp, J. T. *Chem. Rev.* **2012**, *112*, 1105−1125.
(81) Cui, Y.; Yue, Y.; Qian, G.; Chen, B. *Chem. Rev.* **2012**, *112*, 1126−1162.
(82) Campbell, M. G.; Sheberla, D.; Liu, S. F.; Swager, T. M.; Dincă, M. *Angew. Chem., Int. Ed.* **2015**, *54*, 4349−4352.
(83) Shustova, N. B.; Cozzolino, A. F.; Reineke, S.; Baldo, M.; Dincă, M. *J. Am. Chem. Soc.* **2013**, *135*, 13326−13329.
(84) Desai, A. V.; Samanta, P.; Manna, B.; Ghosh, S. K. *Chem. Commun.* **2015**, *51*, 6111−6114.
(85) Xiong, R.; Odbadrakh, K.; Michalkova, A.; Luna, J. P.; Petrova, T.; Keffer, D. J.; Nicholson, D. M.; Fuentes-Cabrera, M. A.; Lewis, J. P.; Leszczynski, J. *Sens. Actuators, B* **2010**, *148*, 459−468.
(86) Nagarkar, S. S.; Joarder, B.; Chaudhari, A. K.; Mukherjee, S.; Ghosh, S. K. *Angew. Chem., Int. Ed.* **2013**, *52*, 2881−2885.
(87) Joarder, B.; Desai, A. V.; Samanta, P.; Mukherjee, S.; Ghosh, S. K. *Chem. - Eur. J.* **2015**, *21*, 965−969.
(88) Nagarkar, S. S.; Desai, A. V.; Ghosh, S. K. *Chem. Commun.* **2014**, *50*, 8915−8918.
(89) Nagarkar, S. S.; Desai, A. V.; Samanta, P.; Ghosh, S. K. *Dalton Trans.* **2015**, DOI: 10.1039/C5DT00397K.
(90) Nagarkar, S. S.; Saha, T.; Desai, A. V.; Talukdar, P.; Ghosh, S. K. *Sci. Rep.* **2014**, *4*, DOI: 10.1038/srep07053.

DOI: 10.1021/acs.cgd.5b00902
Cryst. Growth Des. XXXX, XXX, XXX−XXX

(91) An, J.; Shade, C. M.; Chengelis-Czegan, D. A.; Petoud, S.; Rosi, N. L. *J. Am. Chem. Soc.* **2011**, *133*, 1220−1223.
(92) Gong, Y.-N.; Lu, T.-B. *Chem. Commun.* **2013**, *49*, 7711−7713.
(93) Ma, J.-P.; Yu, Y.; Dong, Y.-B. *Chem. Commun.* **2012**, *48*, 2946−2948.
(94) Hinterholzinger, F. M.; Rühle, B.; Wuttke, S.; Karaghiosoff, K.; Bein, T. *Sci. Rep.* **2013**, *3*.
(95) Jia, Y.; Wei, B.; Duan, R.; Zhang, Y.; Wang, B.; Hakeem, A.; Liu, N.; Ou, X.; Xu, S.; Chen, Z.; Lou, X.; Xia, F. *Sci. Rep.* **2014**, *4*.
(96) Zhu, X.; Zheng, H.; Wei, X.; Lin, Z.; Guo, L.; Qiu, B.; Chen, G. *Chem. Commun.* **2013**, *49*, 1276−1278.
(97) Takashima, Y.; Martínez, V. M.; Furukawa, S.; Kondo, M.; Shimomura, S.; Uehara, H.; Nakahama, M.; Sugimoto, K.; Kitagawa, S. *Nat. Commun.* **2011**, *2*, 168.
(98) Aguilera-Sigalat, J.; Bradshaw, D. *Chem. Commun.* **2014**, *50*, 4711−4713.
(99) Stylianou, K. C.; Heck, R.; Chong, S. Y.; Bacsa, J.; Jones, J. T. A.; Khimyak, Y. Z.; Bradshaw, D.; Rosseinsky, M. J. *J. Am. Chem. Soc.* **2010**, *132*, 4119−4130.
(100) Vishnoi, P.; Walawalkar, M. G.; Sen, S.; Datta, A.; Patwari, G. N.; Murugavel, R. *Phys. Chem. Chem. Phys.* **2014**, *16*, 10651−10658.
(101) Sapchenko, S. A.; Samsonenko, D. G.; Dybtsev, D. N.; Melgunov, M. S.; Fedin, V. P. *Dalton Trans.* **2011**, *40*, 2196−2203.
(102) *SAINT Plus*, v 7.03; Bruker AXS Inc.; Madison, WI, 2004.
(103) Sheldrick, G. M. *SHELXTL, Reference Manual*, v 5.1; Bruker AXS; Madison, WI, 1997.
(104) Sheldrick, G. M. *Acta Crystallogr., Sect. A: Found. Crystallogr.* **2008**, *64*, 112−122.
(105) Farrugia, L.*WINGX* v 1.80.05; University of Glasgow.
(106) Spek, A. L. *PLATON, A Multipurpose Crystallographic Tool*; Utrecht University, Utrecht, The Netherlands, 2005.
(107) Jasuja, H.; Burtch, N. C.; Huang, Y.-g.; Cai, Y.; Walton, K. S. *Langmuir* **2013**, *29*, 633−642.
(108) Jasuja, H.; Jiao, Y.; Burtch, N. C.; Huang, Y.-g.; Walton, K. S. *Langmuir* **2014**, *30*, 14300−14307.
(109) Liu, L.; Telfer, S. G. *J. Am. Chem. Soc.* **2015**, *137*, 3901−3909.
(110) Tan, K.; Nijem, N.; Gao, Y.; Zuluaga, S.; Li, J.; Thonhauser, T.; Chabal, Y. J. *CrystEngComm* **2015**, *17*, 247−260.
(111) Bellarosa, L.; Gutierrez-Sevillano, J. J.; Calero, S.; Lopez, N. *Phys. Chem. Chem. Phys.* **2013**, *15*, 17696−17704.
(112) Guo, P.; Dutta, D.; Wong-Foy, A. G.; Gidley, D. W.; Matzger, A. J. *J. Am. Chem. Soc.* **2015**, *137*, 2651−2657.
(113) Wu, W.; Ye, S.; Yu, G.; Liu, Y.; Qin, J.; Li, Z. *Macromol. Rapid Commun.* **2012**, *33*, 164−171.
(114) Zhao, D.; Swager, T. M. *Macromolecules* **2005**, *38*, 9377−9384.
(115) Pramanik, S.; Zheng, C.; Zhang, X.; Emge, T. J.; Li, J. *J. Am. Chem. Soc.* **2011**, *133*, 4153−4155.
(116) Goel, N.; Singh, U. P. *J. Phys. Chem. A* **2013**, *117*, 10428−10437.

DOI: 10.1021/acs.cgd.5b00902
Cryst. Growth Des. XXXX, XXX, XXX−XXX